



universität
wien

MASTERARBEIT

Titel der Masterarbeit

„Usage of metabolic inhibitors to quantify bacterial and
archaeal activity in meso- and bathypelagic waters of the
North Atlantic“

verfasst von

Benjamin Pontiller BSc

angestrebter akademischer Grad

Master of Science (MSc)

Wien, 2015

Studienkennzahl lt. Studienblatt:

A 066 833

Studienrichtung lt. Studienblatt:

Masterstudium Ökologie

Betreut von:

Univ.-Prof. Dr. Gerhard J. Herndl

TABLE OF CONTENT

ABSTRACT	1
INTRODUCTION.....	3
MATERIAL AND METHODS	6
Study site and sampling	6
Prokaryotic abundance.....	7
Bulk leucine incorporation rates	7
Concentration and latency experiments with inhibitors.....	8
MICRO-CARD-FISH	8
Microscopic image acquisition and evaluation	10
Evaluation of cell-specific leucine uptake rates.....	10
Evaluation of group-specific leucine incorporation rates	11
Calculation of inhibition efficiency, specificity and statistics	11
RESULTS.....	13
Physical and chemical characteristics of sampled water masses	13
Bulk prokaryotic abundance and leucine incorporation.....	14
Testing the bulk inhibition of EMY and GC7.....	15
Qualitative evaluation of treatment-effect on the percentage of leucine-positive cells	17
Cell-specific leucine incorporation determined by MICRO-CARD-FISH.....	17
Group-specific leucine incorporation determined by MICRO-CARD-FISH	18
Group-specific inhibition efficiency and specificity of EMY and GC7	20
DISCUSSION	24
SUMMARY AND CONCLUSIONS.....	27
ACKNOWLEDGEMENTS	28
REFERENCES.....	29
SUPPLEMENTARY MATERIAL	33
ZUSAMMENFASSUNG.....	37
CURRICULUM VITAE	39

ABSTRACT

Domain-specific metabolic inhibitors are useful to quantify the distribution of prokaryotic activity among Bacteria and Archaea in the oceanic water column. Although applied to marine prokaryotic communities in several studies, an in-depth analyses of the specificity of erythromycin (EMY) and N1-guanyl-1,7-diaminoheptane (GC7) to inhibit bacterial and archaeal activity, respectively, has not been done yet. We tested this domain specificity of these two inhibitors on natural prokaryotic assemblages from the North Atlantic. We hypothesized that in EMY-treated samples archaeal activity is obtained, whereas in GC7-treated samples bacterial activity will be measured. Heterotrophic prokaryotic activity was estimated via ³H-leucine incorporation on the bulk and on the single-cell level using catalyzed reporter deposition fluorescence *in situ* hybridization combined with microautoradiography (MICRO-CARD-FISH). In the water masses used for this inhibitor test, the contribution of Bacteria to total DAPI counts ranged from 29 to 47%, while SAR11 comprised 12 to 21% of the DAPI counts, suggesting that SAR11 contributed substantially to bacterial community. The contribution of Thaumarchaeota ranged from 11 to 23% and Euryarchaeota from 2 to 12% of DAPI counts. In EMY-treated samples leucine incorporation was reduced by ~61%. Using single-cell analyses to test the specificity of the inhibitors, GC7 reduced the substrate uptake of Bacteria and Archaea by 39% and 54%, respectively. Hence, we conclude that neither EMY nor GC7 is entirely domain-specific when applied to complex marine prokaryotic communities. Our results, therefore, call for caution when using these inhibitors to assess domain-specific activities.

Keywords: Erythromycin (EMY), N1-guanyl-1,7-diaminoheptane (GC7), MICRO-CARD-FISH, prokaryotes, dark ocean

INTRODUCTION

The world ocean occupies 71% of the earth's surface and a water volume of 1340×10^6 km³, assuming a mean depth of ~3700 m. In terms of volume the Atlantic Ocean is the second largest ocean occupying 24.6% of the world ocean (Shiklomanov & Rodda 2004) and plays a decisive role in regulating the world climate through the formation of major deep-water masses and the Meridional Overturning Circulation (MOC) (Marshall et al. 2001).

Prokaryotes (i.e., Bacteria and Archaea) are dominating the biota of the meso- and bathypelagic waters, with abundances typically decreasing exponentially from 5×10^5 to 4×10^4 cells mL⁻¹ from the surface ocean to the bottom layers (Arístegui et al. 2009). The alpha-proteobacterial clade SAR11 belongs to the most successful microorganisms in the ocean and comprises up to 50% of the surface microbial community (Morris et al. 2002). Furthermore, SAR11 has the potential to contribute significantly to oceanic C, N, P and S cycles due to their high metabolic activity in surface waters (Malmstrom et al. 2004). While the contribution of SAR11 to total prokaryotic abundance decreases with depth, the relative contribution of mesophilic Archaea increases toward the deep-water masses where Euryarchaeota and Thaumarchaeota contribute up to 30% to the total prokaryotic abundance (Karner et al. 2001; Teira et al. 2006a; Varela et al. 2008). More specifically it has been found that Euryarchaeota are dominating the near-surface waters, whereas the relative contribution of Thaumarchaeota increases with depth (Herndl et al. 2005).

Bacteria and Archaea possess a plethora of distinct metabolic pathways while the general differentiation between autotrophic and heterotrophic organisms is based on the utilized carbon source. Initially, heterotrophy was thought to be the exclusive microbial lifestyle in the oxygenated water column of the dark ocean, however, the chemoautotrophic fixation of dissolved inorganic carbon in the meso- and bathypelagic realm of the North Atlantic was recently estimated to be in a similar range as heterotrophic production (Reinthal et al. 2010). This suggests that dissolved inorganic carbon (DIC) fixation might fundamentally contribute to the organic carbon demand of microbial communities in the dark ocean. In addition, mixotrophy is assumed to be widespread particularly in aquatic systems (Eiler 2006; Hügler & Sievert 2011) and part of the biomass production of heterotrophic Bacteria might also be fueled by inorganic carbon intermediates derived from anaplerotic reactions in the tricarboxylic acid (TCA) cycle (Owen et al. 2002; Hesselsoe et al. 2005).

Besides the Calvin-Benson-Bassham (CBB) cycle using the key enzyme ribulose 1,5-bisphosphate carboxylase/oxygenase (RuBisCO), five alternative CO₂-fixation pathways have

been identified thus far (Thauer 2007). A recent study showed that 47% of the Deltaproteobacteria SAR324, 25% of Gammaproteobacteria and 12% of all examined single amplified genomes contain RuBisCO genes, indicative for chemolithotrophy (Swan et al. 2011). In autotrophic Thaumarchaeota, the 3-hydroxypropionate/4-hydroxybutyrate cycle (3-HP/4-HB) or the dicarboxylate/4-hydroxybutyrate cycle (DC/4-HB) pathway have been found to assimilate DIC (Thauer 2007, Berg et al. 2010). In addition, it has been shown that Thaumarchaeota may play a significant role in the first step of nitrification (Francis et al. 2007). The archaeal ammonia monooxygenase subunit alpha (*amoA*) gene abundance outnumbers the bacterial *amoA* gene abundance by 1-3 orders of magnitude in the North Sea and the Atlantic Ocean, suggesting a significant archaeal contribution to the oceanic nitrogen cycle (Wuchter et al. 2007).

Only about four decades ago, the general notion was that the microbial activity in the dark ocean (>500 m depth) is negligible due to slow growth rates caused by the low amount and the poor quality of organic material in the deep sea (Jannasch & Wirsen 1973). This general view has changed in recent years when it became apparent that microorganisms in the meso- and bathypelagic ocean are fairly active (Aristegui et al. 2009). These findings were substantiated with the advent of activity measurements at single-cell resolution such as microautoradiography linked with catalyzed reporter deposition fluorescence *in situ* hybridization (MICRO-CARD-FISH) which allows to visualize the uptake of radiolabeled substrates by different phylogenetic groups (Lee et al. 1999; Teira et al. 2004; Alonso 2012). Single cell analysis was instrumental to show that Archaea play a vital role in the dark ocean's microbial community taking up amino acids or inorganic carbon (Ouverney & Fuhrman 2000; Herndl et al. 2005; Teira et al. 2006b).

MICRO-CARD-FISH is time consuming, which makes it impractical to use this method routinely if one wants to differentiate archaeal from bacterial activity. The use of specific inhibitors offers the possibilities to knock-out one domain while leaving the other one unaffected to determine group-specific production rates (Levipan et al. 2007a), for example.

Metabolic inhibitors or antibiotics are chemicals that cause cell death or inhibit the growth of most microorganisms by affecting the DNA, RNA, cell wall or protein synthesis (Kohanski et al. 2010). Erythromycin (EMY), for example, is physically hampering either the translation of proteins or the translocation of peptidyl tRNAs and it is assumed that EMY affects predominantly the large ribosomal 50S subunit of Bacteria, whereas Archaea remain largely unaffected (Kohanski et al. 2010; Dunkle et al. 2010). Only recently, antibiotics have also been developed for Archaea and it has been shown that diphtheria toxin caused a

relatively specific inhibition of Archaea (Yokokawa et al. 2012). However, diphtheria toxin is expensive thus, alternative inhibitors were tested. In a lab study, the cell cycle of several archaeal extremophiles was arrested by additions of the spermidine analogue N1-guanyl-1,7-diaminoheptane (GC7) (Jansson et al. 2000). GC7 binds within the active center of the enzyme deoxyhypusine synthase (DHS), which has been found in nearly all examined archaeal proteomes and eukaryotes, and inhibits the hypusination pathway thought to be essential for cell proliferation (Park et al. 2010). GC7 has been proposed as a less expensive and efficient alternative inhibitor for Archaea allowing incubations in larger volumes (Levipan et al. 2007a,b; Farías et al. 2009). Generally, the knowledge on the specificity of metabolic inhibitors is based mainly on a few culture experiments with simple community composition (Jansson et al. 2000; Löscher et al. 2012; Berg et al. 2014a) and has not been extensively studied in complex natural microbial assemblages.

The objective of this study was 1) to test the specificity of the two widely used inhibitors EMY and GC7 on natural complex prokaryotic assemblages throughout the water column of the North Atlantic and 2) to determine the relative contribution of Bacteria and Archaea on the bulk heterotrophic microbial activity. We measured bulk heterotrophic activity via ³H-leucine incorporation and used MICRO-CARD-FISH combined with automated cell counting to evaluate the single cell activity of Bacteria and Archaea. While the bulk measurements suggested selective inhibition of microorganisms, the single cell analyses revealed that EMY and particularly GC7 are not sufficiently specific to allow a clear differentiation of bacteria from archaeal activity by using these two inhibitors.

MATERIAL AND METHODS

Study site and sampling

Sampling was conducted during the MEDEA-2 cruise aboard the RV *Pelagia* in June and July 2012 in the North Atlantic Ocean (Fig. 1). Water samples were taken at seven stations between 49°N and 64°N in different water masses (see Table 1) using a conductivity-temperature-depth (CTD) rosette sampler holding 19 Niskin bottles of 25 L each.

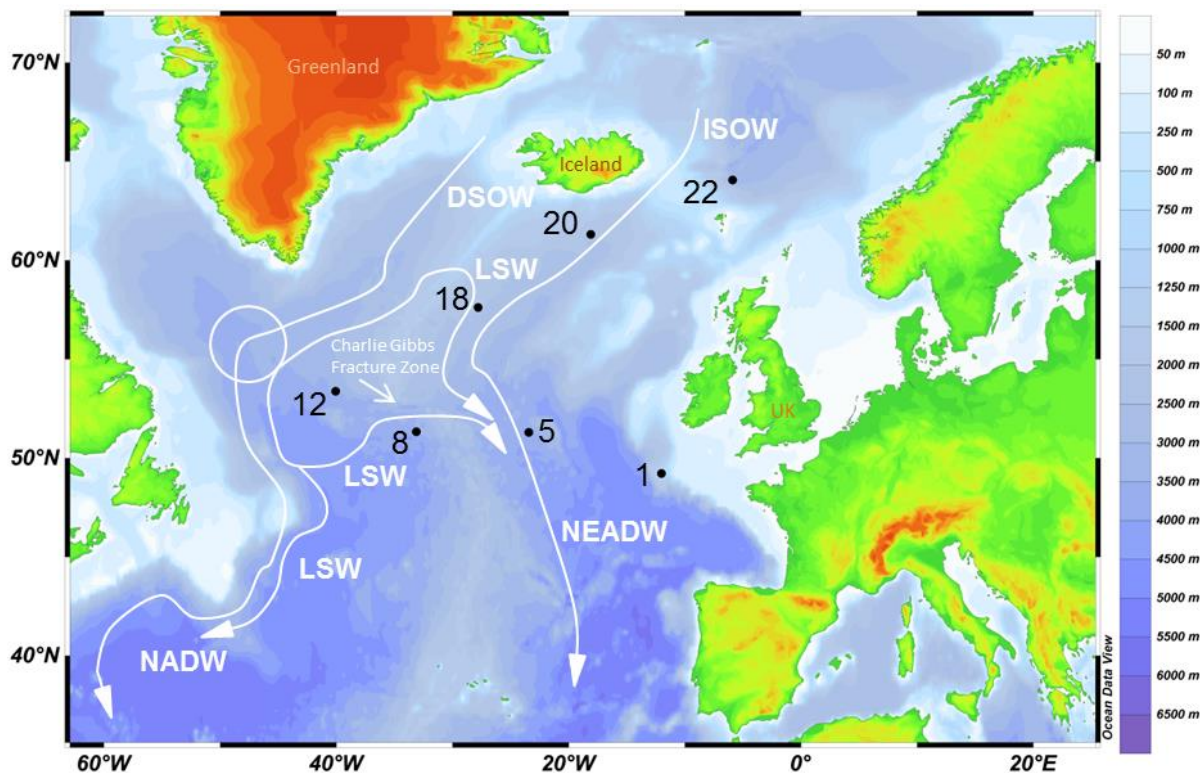


Figure 1: Map of the sampled stations in the North Atlantic. Samples were retrieved at seven stations during the MEDEA-2 cruise in June/July 2012. White lines indicate the simplified flow pattern of major water masses in the North Atlantic. Iceland Scotland Overflow Water (ISOW), Denmark Strait Outflow Water (DSOW), LSW (Labrador Sea Water), North Atlantic Deep Water (NADW), North East Atlantic Deep Water (NEADW).

Prokaryotic abundance

Prokaryotic abundance was enumerated following Marie et al. (1999). Duplicate seawater samples were fixed with glutaraldehyde (final concentration 0.5%) stored in the dark at room temperature for 10 min, flash-frozen and stored at -80°C until analysis on a flow cytometer (BD ACCURI C6, BD Biosciences). Thawed samples (250 µL) were diluted with 0.2-µm filtered TE-buffer in a ratio of 1:1, 5 µL SYBRGreen I was added and samples were incubated at room temperature in the dark for 10 min. Subsequently, cell enumeration was performed by calculating the flow rate of 1 µm fluorescent microspheres of known concentration at 488 nm excitation wavelength (Solid State Blue Laser) and standard filter setup (533/30 nm). Cytogram plots of side scatter versus fluorescence were used to identify prokaryotes. The cell counts were normalized to the fluorescence of microspheres to minimize variability between samples.

Bulk leucine incorporation rates

Bulk leucine incorporation was measured as described in Reinthaler et al. (2010). Briefly, triplicate life samples of 50 mL and 2 formaldehyde killed blanks (final concentration 2%) were spiked with ³H-leucine (final concentration 10 nM, specific activity 120 mCi mmol⁻¹, NEN) and incubated at *in situ* temperature in the dark for 1-24 h depending on the sampling depth. Thereafter, samples were filtered onto 0.2-µm polycarbonate filters (Nuclepore, Whatman) supported with 0.45-µm cellulose nitrate filters (HAWP, Millipore). The filters were rinsed twice with 5% ice-cold trichloroacetic acid (ACS-grade, Sigma-Aldrich), transferred into 20 mL scintillation vials and dried. Eight mL of scintillation cocktail (FilterCount, Canberra-Packard) was added and after an incubation for ~18 h to stabilize fluorescence, the samples were counted in a liquid scintillation counter (Tricarb 3100TR, Perkin Elmer). The leucine incorporation rate was calculated using the mean disintegrations per minute (dpm) of the triplicate life samples corrected by the mean dpm of the duplicate blanks. The dpm were corrected for quenching with internal and external standards.

Concentration and latency experiments with inhibitors

The appropriate concentration and incubation time before adding the radiolabel was tested at Stations 1 and 5 at 831 m and 700 m depth, respectively. To aliquots of 20 mL seawater samples, EMY or GC7 was added at different final concentrations: EMY was tested with concentrations of either 0.3 mmol L⁻¹ or 0.7 mmol L⁻¹, GC7 was tested with concentrations of 0.1 mmol L⁻¹ and 1.0 mmol L⁻¹. An antibiotic-free control received no inhibitors. At all concentrations including the blank, a pre-incubation period of the antibiotic of 30 min or 60 min was tested before adding the ³H-leucine. After subsequent incubation for ~24 h at *in situ* temperature in the dark, the samples were processed as described above for the bulk incorporation measurements. These experiments revealed that using the high concentrations and 60 min pre-incubation time for both inhibitors resulted in the highest inhibition of activity (Fig. 3).

MICRO-CARD-FISH

Seawater for catalyzed reporter deposition fluorescence *in situ* hybridization combined with microautoradiography (MICRO-CARD-FISH) was collected into 500 mL polycarbonate bottles directly from the CTD. To reach an adequate cell abundance on the filters, between 20 mL and 50 mL (depending on the sampling depth) of the seawater was aliquoted into plastic tubes (Greiner Bio one) and 0.7 mmol L⁻¹ of EMY or 1 mmol L⁻¹ of GC7 added to triplicate life samples and one formaldehyde killed control. After a pre-incubation time of 60 min for both inhibitors, ³H-leucine was added at a final concentration of 10 nmol L⁻¹. The samples were incubated in the dark at *in situ* temperature for 1-24 h and subsequently, activity was terminated by adding formaldehyde (final concentration 2%). All fixed samples were incubated for 18 h at 4°C, filtered onto 0.2-µm polycarbonate filters (GTTP, Millipore) and rinsed twice with particle-free Milli-Q water. The filters were dried completely and stored in 1.5 mL microcentrifuge vials at -80°C until further processing in the laboratory.

MICRO-CARD-FISH was performed according to Teira et al. (2004). The filters were thawed and embedded in 0.1% low-gelling-point agarose and subsequently dried at 37°C for 10 min. The cell-wall permeabilization was done with either lysozyme (10 mg mL⁻¹, 37°C, 1 h) or HCl (0.1 mol L⁻¹, 20°C, 1 min) for Bacteria and Archaea, respectively. Hybridization was performed with horse radish peroxidase (HRP)-labeled probes specific for Bacteria, SAR11, Thaumarchaeota and Euryarchaeota and additionally with Non-EUB338 (for probe sequences and hybridization conditions see Table S2) supplied at a ratio of 1:20 of probe to

hybridization buffer. Hybridization was conducted at 35°C for 16 h under dark conditions in continuously rotating vials (5 rpm min⁻¹). Signal amplification was performed by incubating the filters in a substrate mix of 1:100 dilution of tyramides linked to the fluorescent dye Atto488 in an amplification buffer under the presence of H₂O₂ (final conc. 0.0015%), at 37°C for 40 min (see detailed protocol in the supplementary material and methods).

In a darkroom, the hybridized filters were transferred onto pre-cleaned microscopic glass slides coated with ~10 µm photographic emulsion and incubated for a previously determined time. We used the Kodak NTB2 photographic emulsion until Kodak ceased the supply. The experiments for Thaumarchaeota and Euryarchaeota of Stn 12 (subsurface layer, ≈100 m depth, SSL), Stn 8, 12 and 22 (O₂-min layer, ≈450 m) were conducted with the Kodak NTB2 emulsion, while the remaining experiments were conducted with the Ilford K.5 (Ilford PHOTO, England). The emulsion was diluted in a 1:1 ratio with Milli-Q and pre-warmed at 40°C for 1 h prior to coating the slides. Both emulsions revealed similar sensitivity according to tests with aliquots of some samples. The coated slides were dried briefly on an aluminum plate placed on ice. In the dark, filter sections were transferred onto the emulsion and thereafter, placed in a light-tight box containing silica-beads.

In order to test the required exposure time for microautoradiography, two samples with high ³H-leucine and ¹⁴C-sodium bicarbonate incorporation rates were used (see supplementary Fig. S3A and S3B). These tests indicated that an exposure time of 6 - 8 days is sufficient. Consequently, the slides were incubated horizontally at 4°C for 6-8 days depending on the activity based on tests considering dpm counts and exposure time as well as screening of filter sections for activity without prior hybridization. Following incubation, the slides were processed according to Ilford specifications using Ilford Phenisol, Ilfostop and Rapid Fixer (Ilford Photo, England).

To prevent systematic variation between the three treatments (Control, EMY and GC7) due to handling, emulsion thickness or emulsion age, the treatments of each probe were incubated on the same slide. After developing and fixing the photographic emulsion, peeling of the filter sections was done as described in Samo et al. (2014) using a cold spray (Cold 75 Super; CRC Industries Europe BVBA). The cells were counter-stained and mounted in a DAPI-mix containing PBS, 1 µg mL⁻¹ of 4',6-diamino-2-phenylindole, Vectashield (Vector Laboratories, Inc.) and Citifluor (Citifluor, Ltd.).

Microscopic image acquisition and evaluation

Microscopy was performed on a Zeiss Axio Imager M2 epifluorescence microscope (Carl Zeiss), with a filter set for Atto488 and DAPI. The silver grain halos (indicative for uptake of the radiolabeled tracer) around stained cells were detected by switching from the epifluorescence mode into the transmission mode. Pictures were taken manually with a Plan-Apochromat 100x/1.46 oil objective lens and an AxioCam MRm black and white high-resolution camera (Carl Zeiss).

For each filter section, ~10 pictures were taken for each filter set (DAPI and Atto488) as well as in the transmission mode yielding a total ~120 pictures per slide. A set of 3 pictures was overlain and the pixels were evaluated by using the custom made software DotAre (Frank et al. in prep.). More than 300 DAPI-stained cells were counted per sample. The software parameters were optimized with a training set of 10 manually counted pictures using the whole range of possible configurations. Microbial cells were classified as probe positive if a DAPI-stained cell showed a fluorescence signal of the specific hybridization probe. Probe negative cells were visibly stained with DAPI only. Additionally, all fluorescence signals were checked for surrounding silver grain halos. The minimum requirement to assign an area to cell activity was a complete overlap between cell and silver grain halo. Thus, the random background noise was reduced. If cells had overlapping silver grain halos, the activity was weighted based on the distance between the cells and the center of the halo. Cells with Atto488 fluorescence but unrecognized DAPI signal were also classified as active probe positive cells, the percentage of these probes with silver-grain halo was overall < 10%. The hybridization with the Non-EUB338 probe to determine the percentage of unspecific binding yielded $1.4\% \pm 0.4\%$ (mean \pm SD, $n = 13$) probe positive signals and $3.7\% \pm 1.6\%$ ($n = 13$) probe negative signals.

Evaluation of cell-specific leucine uptake rates

To calculate the leucine incorporation per cell, we normalized the bulk leucine uptake per filter to the total cell-bound silver grain area which was scaled to the same filter area. Subsequently, the obtained ratio ($\text{nmol d}^{-1} \mu\text{m}^{-2}$) was multiplied with the silver grain area associated with determined probe-positive cells and normalized to the cell abundance on the filter area resulting in an average probe-positive cell-specific leucine uptake rate per day ($\text{mol leucine cell}^{-1} \text{d}^{-1}$).

Evaluation of group-specific leucine incorporation rates

We calculated the group-specific activity based on the counts of active cells and the area of the silver-grain halos. The cell-specific activity-count was calculated as the sum of probe-positive cells surrounded by a silver-grain halo. The group-specific activity-count was determined as the sum of active probe-positive cells. To obtain the group-specific activity, the silver-grain halo-area was normalized to picture counts to correct for the number of pictures taken. Thereafter, the bulk leucine incorporation assessed by liquid scintillation counting was used as a quantitative reference and divided by the cell-bound silver-grain halo to obtain the cell-bound activity per pixel ($\text{nmol leu m}^{-3} \text{ d}^{-1} \text{ px}^{-1}$) and multiplied with the probe-positive cell-specific silver grain halo area to determine the probe-positive cell-specific leucine incorporation ($\text{nmol m}^{-3} \text{ d}^{-1}$). Finally, the sum of Bacteria-, Thaumarchaeota- and Euryarchaeota-specific leucine incorporation was scaled to the measured bulk leucine incorporation.

The abundance of specific prokaryotic groups, obtained with MICRO-CARD-FISH, is given as percentage of total DAPI counts. The Gaussian error propagation was used to calculate the total error of Bacteria and Archaea in Figure 2.

Calculation of inhibition efficiency, specificity and statistics

To account for the filter- associated variability of total probe-positive cells we normalized the activity based on the encountered probes in each treatment via the probe-specific activity (PSA):

$$PSA = \frac{P_a}{P_t} \tag{1}$$

where P_a is either the count of active probe-positive cells, resulting in the PSA_c or the silver grain halo area, which results in the PSA_a and P_t is the total number of probe-positive cells calculated for each treatment and both calculations.

To calculate the inhibition efficiency (IE), we used the PSA of each inhibitor (PSA_{treat}) and the untreated sample (PSA_{ctrl}):

$$IE = \frac{PSA_{treat}}{PSA_{ctrl}} * 100\% \quad (2)$$

To calculate the inhibition specificity (IS) for both inhibitors, the determined IE based on cell counts and silver grain halo area was used since we expect both to add different aspects of information:

$$IS = \frac{IE_{TG} - IE_{NTG}}{IE_{NTG}} \quad (3)$$

Assuming that EMY specifically inhibits Bacteria but not Archaea, we considered Bacteria as the target group (TG) and Archaea as the non-target group (NTG). GC7 is assumed to be a specific inhibitor of Archaea and Eukaryotes, while Bacteria should be unaffected. Consequently, in the case of GC7 Archaea are the TG and Bacteria the NTG.

We controlled all samples for a possible treatment-related or a non-random cell-loss-effect during the peeling of the filter after microautoradiography. Therefore, we determined the relative abundance of Bacteria and Thaumarchaeota, for each treatment separately and analyzed the ratio of Bacteria to Thaumarchaeota probe counts using one-way analysis of variance (ANOVA). All statistical prerequisites for ANOVA were tested and met. All statistical analyses were conducted with SigmaPlot Version 11.

RESULTS

Physical and chemical characteristics of sampled water masses

The physical and chemical characteristics of the different water masses are given in Table 1. Overall, in our study area temperature ranged from 11°C to -0.8°C. Generally, the highest water temperature was measured in the SSL and O₂-min, and increased from ~2°C to ~11°C from the North to South, respectively. The temperature of the Upper Labrador Sea Water (ULSW) was ~4°C, while the coldest water temperature -0.8°C was measured in the Norwegian Sea Deep Water (NSDW) at 3200 m depth (Table 1).

Table 1: Locations of the occupied stations (Stn) and the physical and chemical characteristics of sampled water masses (WM) in the northern North Atlantic.

WM ^a	Stn	Lat [°N]	Long [°E]	Depth [m]	Temp. [°C]	Sal	σ_0 [kg m ⁻³]	NH ₄ [μM]	NO ₃ [μM]	PO ₄ [μM]	Si [μM]
SSL	22	64.07	354.10	99	3.37	34.93	27.80	0.47	10.39	0.74	4.15
	20	61.32	341.89	99	8.95	35.20	27.28	0.13	12.62	0.82	4.39
	18	57.62	332.19	99	8.34	35.03	27.25	0.14	13.59	0.88	5.44
	12	53.38	319.93	99	5.48	34.79	27.45	0.15	18.76	1.18	10.02
	8	51.34	326.87	98	11.01	35.23	26.95	0.14	9.54	0.63	4.08
O ₂ -min	22	64.07	354.10	248	1.91	34.97	27.96	0.08	13.73	0.92	5.47
	20	61.32	341.89	726	7.05	35.15	27.54	0.11	18.27	1.18	10.07
	12	53.38	319.93	495	4.03	34.88	27.69	0.13	16.59	1.09	8.45
	5	51.30	336.55	689	8.90	35.28	27.36	NA	NA	NA	NA
	1	49.23	347.98	823	9.94	35.63	27.47	NA	NA	NA	NA
ULSW	20	61.32	341.89	988	5.15	35.01	27.68	0.10	18.44	1.20	10.90
	12	53.38	319.93	989	3.72	34.89	27.73	0.13	17.09	1.11	9.68
	8	51.34	326.87	1086	4.04	34.92	27.73	0.08	17.28	1.12	10.05
NSDW	22	64.07	354.10	3137	-0.79	34.91	28.08	0.05	15.69	1.04	14.07

^a Abbreviations of water masses: Subsurface layer (SSL), Oxygen minimum zone (O₂-min), Upper Labrador Sea Water (ULSW), Norwegian Sea Deep Water (NSDW), No data (NA).

Bulk prokaryotic abundance and leucine incorporation

In general, the prokaryotic abundance was highest in the SSL (range $4.1 - 2.2 \times 10^5$ cells mL⁻¹) and lowest in the NSDW (5.9×10^4 cells mL⁻¹). Generally, higher cell abundance was obtained by flow cytometry (range $4.1 \times 10^5 - 5.9 \times 10^4$), while abundances obtained with CARD-FISH were ~38% and with MICRO-CARD-FISH ~77% lower compared to flow cytometry (Fig. S1A).

Similar to the total cell abundance, the leucine uptake of the bulk community decreased exponentially with depth (Fig. S1B). The highest uptake of radiolabeled leucine was measured in the SSL (51.6 ± 32.8 nmol leu m⁻³ d⁻¹, n = 5). Leucine uptake declined towards the O₂-min (11.5 ± 6.2 nmol leu m⁻³ d⁻¹, n = 4) and was low in the ULSW (1.9 ± 0.5 nmol leu m⁻³ d⁻¹, n = 3) and the NSDW (1.3 nmol leu m⁻³ d⁻¹, n = 1) (Fig. S1B).

Bacterial and archaeal abundance and community composition

The relative abundance of Bacteria measured with MICRO-CARD-FISH was $43.1 \pm 7.2\%$ (n = 8) in the epi- and upper mesopelagic water masses, while the relative abundance declined with depth to $29.2 \pm 24.2\%$ (n = 3) in the ULSW and to 28.6% (n = 1) of DAPI stained cells in the NSDW of the Arctic Ocean. However, the relative contribution of the α -proteobacterial clade SAR11 was rather constant throughout the water column ($18.1\% \pm 9.8\%$ of DAPI stained cells, n = 12) (Fig. 2).

The relative abundance of Thaumarchaeota increased with depth from $10.5\% \pm 4.2\%$ (n = 5) in the SSL to 23.2% (n = 1) in the NSDW (Fig. 2). Generally, the contribution of Euryarchaeota to total DAPI counts was rather constant throughout the water column with an average of $2.5\% \pm 1.7\%$ (n = 11). Euryarchaeota in the NSDW of the Arctic Ocean exhibited a relative abundance of 11.5% (n = 1) of DAPI stained cells.

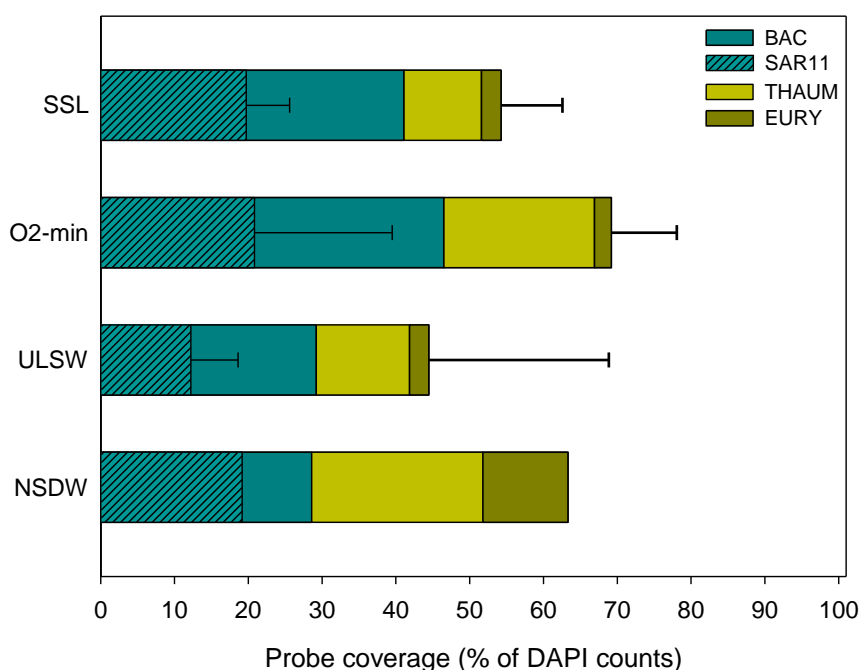


Figure 2: Community composition obtained by MICRO-CARD-FISH. The probe coverage was calculated as the percentage of the specific fluorescent probe compared to the total DAPI counts. Error bars indicate the standard deviation of the mean values of SAR11 and the total error of counting Bacteria, Thaumarchaeota and Euryarchaeota. SSL (n = 5), O₂-min (n = 4), ULSW (n = 3), NSDW (n = 1). For water mass abbreviations see Table 1.

Testing the bulk inhibition of EMY and GC7

Samples treated with 0.3 mmol L⁻¹ EMY and pre-incubated for 30 min yielded a leucine incorporation rate of 28.4 nmol leu m⁻³ d⁻¹ (range: 20.5 – 36.4 nmol leu m⁻³ d⁻¹, n = 2) and after 60 min pre-incubation, leucine incorporation was slightly higher at 33.0 nmol leu m⁻³ d⁻¹ (range: 29.3 – 36.8 nmol leu m⁻³ d⁻¹, n = 2) (Fig. 3A). With a pre-incubation time of 30 min and EMY additions of 0.7 mmol L⁻¹ the substrate incorporation was 22.6 nmol leu m⁻³ d⁻¹ (range: 15.5 – 29.8 nmol leu m⁻³ d⁻¹, n = 2) and after pre-incubating the samples for 60 min, leucine incorporation was 25.8 nmol leu m⁻³ d⁻¹ (range: 21.3 – 30.2 nmol leu m⁻³ d⁻¹, n = 2) (Fig. 3A).

Addition of 0.1 mmol L⁻¹ of GC7 and a pre-incubation time of 30 min resulted in an incorporation of 90.4 nmol leu m⁻³ d⁻¹ (range: 71.2 – 109.6 nmol leu m⁻³ d⁻¹, n = 2) and after 60 min of pre-incubation time in 85.9 nmol leu m⁻³ d⁻¹ (range: 61.0 – 110.8 nmol leu m⁻³ d⁻¹, n = 2). Using 1 mmol L⁻¹ of GC7 addition, leucine incorporation after 30 min resulted in a leucine incorporation of 71.9 nmol leu m⁻³ d⁻¹ (range: 53.9 – 89.8 nmol leu m⁻³ d⁻¹, n = 2) and after 60 min 64.1 nmol leu m⁻³ d⁻¹ (range: 48.8 – 79.4 nmol leu m⁻³ d⁻¹, n = 2) (Fig. 3A).

Hence, the highest inhibition of the *in situ* bulk leucine incorporation was achieved by using a combination of 30 min pre-incubation with the highest tested concentration of EMY (0.7 mmol L⁻¹) and 60 min for GC7 (1 mmol L⁻¹) (Fig. 3A). In addition, a sample of Station 5 (700 m depth) was spiked with both inhibitors at highest concentrations (EMY, 0.7 mmol L⁻¹ and GC7, 1 mmol L⁻¹) and a pre-incubation time of 60 min was applied. The leucine incorporation was 27.7 nmol leu m⁻³ d⁻¹ and similar to the 0.7 mmol L⁻¹ in the EMY-treated sample with 25.8 nmol leu m⁻³ d⁻¹ (Fig. 3A). In these experiments the untreated control yielded a bulk leucine incorporation of 111.8 nmol leu m⁻³ d⁻¹ (range: 79 - 144 nmol leu m⁻³ d⁻¹, n = 2) (Fig. 3A).

The inhibitors EMY and GC7 were also tested on the bulk community in the different water masses (Fig. 3B). In general, inhibition was rather constant over the different water masses for both inhibitors. The percentage of leucine incorporation in samples collected from the different water masses and treated either with EMY or GC7 in relation to the leucine incorporation obtained in the untreated samples is shown in Fig. 3B. Averaged over the individual water masses, in samples treated with EMY, leucine incorporation was reduced to 23 ± 9% of the leucine incorporation in the untreated water masses while in the GC7-treated samples leucine incorporation amounted to 59 ± 10% (n = 13) of that in the untreated water masses (Fig. 3B).

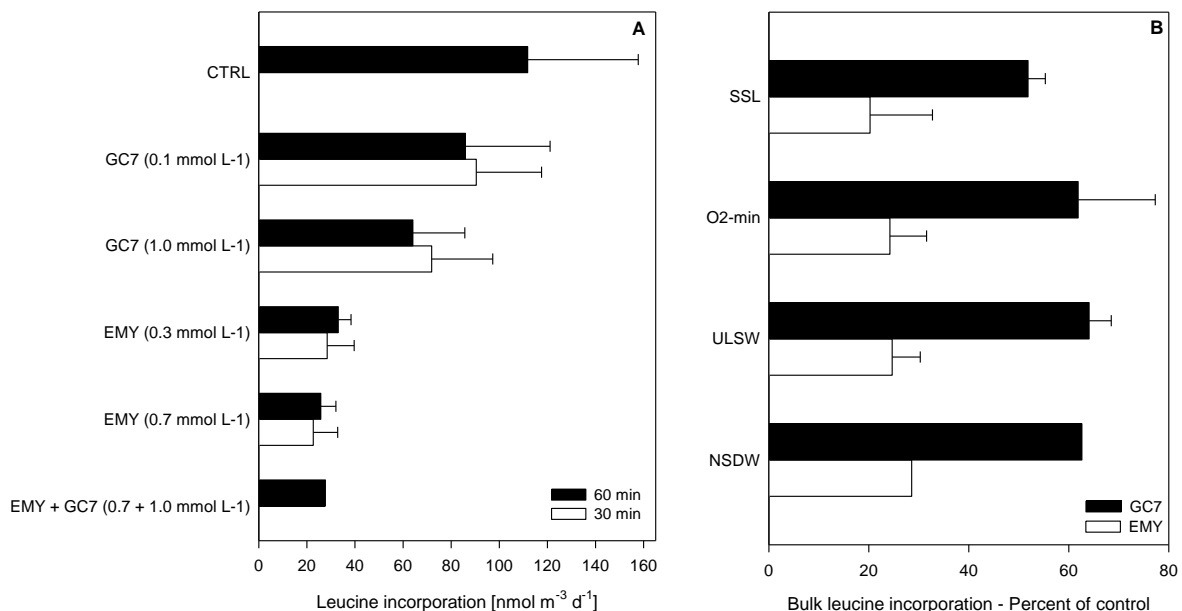


Figure 3: Bulk leucine incorporation of (A) different concentrations and incubation times of EMY and GC7, whiskers indicate the range of the duplicates; (B) water-mass associated samples treated with either EMY or GC7 using a pre-incubation time of 60 min and highest concentrations as indicated in the left panel. Error bars indicate the standard deviation of the mean, SSL (n = 5), O₂-min (N = 4), ULSW (n = 3), NSDW (n = 1). For water mass abbreviations see Table 1.

Qualitative evaluation of treatment-effect on the percentage of leucine-positive cells

The enumeration of cells taking up leucine ranged between 39.7% and 47.9% throughout the water column in the untreated control (Table 2). In general, a lower percentage of leucine-positive cells was obtained in samples treated with EMY (range: 21.4% - 36.9%) than with GC7 (range: 39.4% - 41.6%). The addition of EMY reduced the percentage of active cells (range: 8.4% - 54.5%) and GC7 (range: -3.2% - 33.8%) compared to unamended controls (Table 2).

TABLE 2: Overview of leucine-positive cells to total cell counts in %.

WM ^a	CTRL			EMY			GC7		
	Mean	±SD	n	Mean	±SD	n	Mean	±SD	n
SSL	47.4	9.7	20	26.3	16.8	20	31.4	10.9	20
O ₂ -min	47.9	12.4	16	21.8	9.2	14	39.4	6.9	15
ULSW	40.3	14.9	12	36.9	9.6	11	41.6	14.6	11
NSDW	39.7	7.1	4	21.4	6.5	4	39.4	6.9	4

^aFor abbreviation of water masses see Table 1, ±SD - standard deviation of the mean, n – number of measurements.

Cell-specific leucine incorporation determined by MICRO-CARD-FISH

The cell-specific leucine incorporation of samples treated either with EMY or GC7 in relation to the unamended control is shown in Table 3. In general, the per-cell activity of Bacteria and Archaea in the untreated control decreased with depth (Table 3). The highest cell-specific leucine incorporation was obtained in the SSL for Bacteria (6.3×10^{-20} mol leucine cell⁻¹ d⁻¹) and SAR11 (5.6×10^{-20} mol leucine cell⁻¹ d⁻¹), while the highest per-cell activity of Thaumarchaeota (25×10^{-20} mol leucine cell⁻¹ d⁻¹) was obtained in the O₂-min and of Euryarchaeota in the SSL (4.1×10^{-20} mol leucine cell⁻¹ d⁻¹).

In the SSL, we obtained for EMY-treated samples a bacterial per-cell substrate uptake of 2.1×10^{-20} mol leucine cell⁻¹ d⁻¹ and of Thaumarchaeota 0.5×10^{-20} mol leucine cell⁻¹ d⁻¹ (Table 3). Hence, EMY affected the per-cell activity of Bacteria and Thaumarchaeota similarly. Generally, GC7 reduced the per-cell substrate incorporation of Bacteria (5.6×10^{-20} mol leucine cell⁻¹ d⁻¹) and Thaumarchaeota (1.1×10^{-20} mol leucine cell⁻¹ d⁻¹) less efficiently

than EMY, albeit both groups were affected. These findings highlight the relatively low specificity of GC7 at the single-cell level for Archaea (Table 3; Fig. 5).

In some samples the obtained per-cell leucine incorporation rates of the treatments were higher than those of the unamended controls (Table 3).

TABLE 3: Cell-specific leucine incorporation [$\times 10^{-20}$ mol cell⁻¹ d⁻¹].

WM ^a	Probe	CTRL			EMY			GC7		
		Mean	±SD	n	Mean	±SD	n	Mean	±SD	n
SSL	Bacteria	6.3	3.2	5	2.1	2.3	5	5.6	3.2	5
	SAR11	5.6	4.2	5	2.7	4.4	5	2.1	1.6	5
	Thaumarchaeota	2.2	1.8	5	0.5	0.4	5	1.1	0.8	5
	Euryarchaeota	4.1	2.4	5	3.5	7.4	5	5.8	5.5	5
O ₂ -min	Bacteria	2.4	1.6	4	0.5	0.2	4	0.9	0.6	4
	SAR11	2.4	0.4	4	0.4	0.3	4	0.7	0.5	4
	Thaumarchaeota	25.3	49.0	4	0.2	0.2	4	0.3	0.3	4
	Euryarchaeota	2.9	2.7	4	0.6	0.6	4	1.5	0.7	4
ULSW	Bacteria	1.4	1.0	3	0.4	0.1	2	12.1	16.5	3
	SAR11	1.2	0.9	3	0.3	0.2	3	0.4	0.4	3
	Thaumarchaeota	0.1	0.0	3	0.1	0.1	3	3.3	4.8	3
	Euryarchaeota	0.7	0.6	3	0.7	0.8	3	1.0	0.7	3
NSDW	Bacteria	1.7	ND	1	16.0	ND	1	1.0	ND	1
	SAR11	2.6	ND	1	1.3	ND	1	0.8	ND	1
	Thaumarchaeota	0.1	ND	1	0.1	ND	1	0.2	ND	1
	Euryarchaeota	0.6	ND	1	0.2	ND	1	0.4	ND	1

^a For abbreviation of water masses (WM) see Table 1, ND – Not determined, ±SD - standard deviation of the mean, n – number of measurements.

Group-specific leucine incorporation determined by MICRO-CARD-FISH

To examine the group-specificity of both inhibitors, we measured the leucine incorporation in the untreated controls and either EMY- or GC7-treated samples. In the uninhibited control, leucine uptake decreased with depth (Fig. 4A). In the SSL, leucine incorporation of Bacteria was 46.3 nmol leu m⁻³ d⁻¹ with almost half of the bacterial activity due to SAR11. Bacterial leucine uptake decreased to 8.7 nmol leu m⁻³ d⁻¹ in the O₂-min, where 60% of the bacterial leucine uptake was mediated by SAR11 (Fig. 4A). The lowest bacterial activity was obtained in the ULSW of the bathypelagic (1.7 nmol leu m⁻³ d⁻¹) and in the NSDW of the Arctic Ocean (1.0 nmol leu m⁻³ d⁻¹). Similarly, leucine uptake of SAR11

followed the general declining trend with depth, albeit SAR11 contributed about 50% to bacterial leucine uptake throughout the water column (Fig. 4A).

Also archaeal leucine uptake declined with depth (Fig. 4A). Thaumarchaeota contributed about twice as much to leucine uptake ($3.8 \text{ nmol leu m}^{-3} \text{ d}^{-1}$) than Euryarchaeota ($1.5 \text{ nmol leu m}^{-3} \text{ d}^{-1}$) in the SSL (Fig. 4A). In the O_2 -min zone, leucine uptake by Archaea decreased to approximately one-third of that in the SSL ($1.2 \text{ nmol leu m}^{-3} \text{ d}^{-1}$ for Thaumarchaeota, $0.6 \text{ nmol leu m}^{-3} \text{ d}^{-1}$ for Euryarchaeota). Both archaeal groups showed the lowest leucine uptake ($0.1 \text{ nmol leu m}^{-3} \text{ d}^{-1}$) in the ULSW (Fig. 4A).

As bulk leucine incorporation decreased in both treatments (EMY and GC7), we determined the relative contribution of the individual prokaryotic groups to the remaining activity. Overall, we did not detect an obvious change in the relative contribution of each group to the total leucine uptake (Fig. 4, Fig. S2). Nevertheless, the apparent decrease in overall activity (Fig. 3, Table 2, Table 3 and Fig. 4) and the distribution of the activity within the community seemed to remain fairly constant (Fig. S2). Addition of EMY to O_2 -min samples resulted in a remaining Bacteria-associated leucine uptake of 20.2% of the originally measured $10.5 \text{ nmol m}^{-3} \text{ d}^{-1}$ of the control. Similarly, the activity mediated by SAR11 was 9.1% of the total leucine uptake in the unamended control (Fig. 4B, Table S1). Remarkably, the addition of EMY affected also Archaea. The remaining thaum- and euryarchaeotal activity was 2.5% and 3.0%, respectively, of the total activity in the respective control.

Similar to EMY, the addition of GC7 also reduced the leucine uptake of Bacteria in O_2 -min samples (Fig. 4C). The remaining bacterial leucine uptake in GC7-treated samples was 48.9% of the unamended control and only 7.3% for SAR11 (Fig. 4C). In the GC7-treated samples, the remaining leucine uptake of Thaum- and Euryarchaeota was only 9.4% and 5.6%, respectively, of the corresponding leucine uptake in the unamended samples (Fig. 4C).

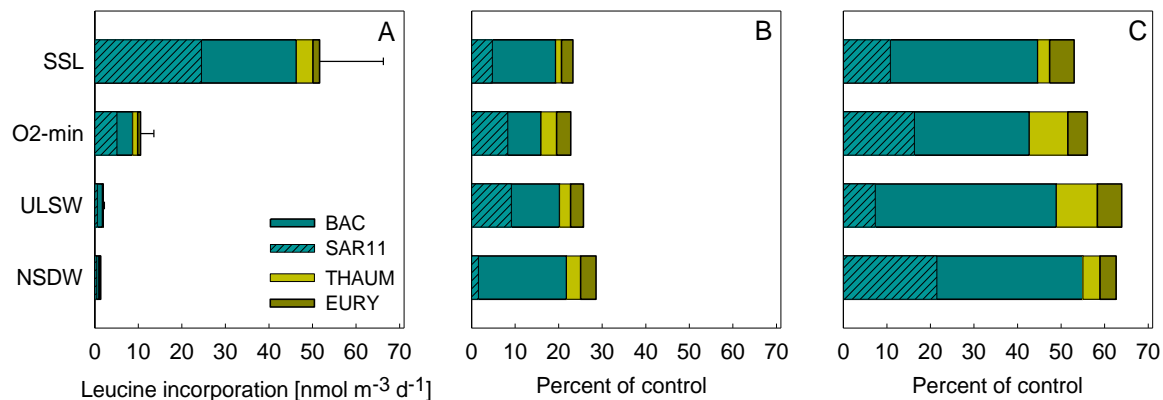


Figure 4: (A) Group-specific leucine incorporation of the control, (B) remaining leucine incorporation of EMY - treated samples and (C) of GC7 - treated samples, expressed as the percentage of control. The error bars show the standard error of the bulk leucine incorporation. Further details are given in the supplementary (Fig. S2). For water mass abbreviations and numbers of determinations see Table 1.

Group-specific inhibition efficiency and specificity of EMY and GC7

The inhibition efficiency (IE) of both inhibitors was assessed for both phylogenetic groups (Bacteria and Thaumarchaeota) based on the probe specific activity (PSA) as defined in Material and Methods. Euryarchaeota were excluded, owing to their relatively low abundance and very low leucine incorporation rates in the controls, which made calculations of IE rather stochastic.

For EMY, we determined an IE for Bacteria of $42.4 \pm 21.4\%$ ($n = 10$) and for Thaumarchaeota of $45.7 \pm 22.9\%$ ($n = 10$) throughout the water column (Table 4). The IE for Bacteria and Thaumarchaeota was similar in the epi- and upper mesopelagic ($50.2 \pm 19.9\%$; $n = 15$). In the ULSW the IE ranged between 22.5 and 38.2% ($n = 2$) for Bacteria and between 6.3 and 51.9% ($n = 2$) for Thaumarchaeota, respectively. The lowest IE of 9.7% was calculated for Bacteria in the NSDW (Table 4).

For GC7, the overall IE for Bacteria was $28.6 \pm 10.4\%$ ($n = 10$) and for Thaumarchaeota $47.1 \pm 25.5\%$ ($n = 8$). In the SSL, the bacterial IE was $34.9 \pm 7.9\%$ ($n = 4$) and in the mesopelagic of the North Atlantic and the upper bathypelagic of the Arctic Ocean $24.3 \pm 10.2\%$ ($n = 6$). Generally, higher inhibition was obtained for Thaumarchaeota with $53.0 \pm 22.7\%$ ($n = 4$) in the SSL and $41.3 \pm 30.1\%$ ($n = 4$) in the O₂-min and ULSW (Table 4).

Since determination of activity based on binary numbers (PSA_c, non-active/active) is only a qualitative approach, we additionally calculated the IE of EMY based on the probe specific activity (PSA_a) obtained from the area of the silver-grain halo (see Material and

Methods). Using this metric approach for EMY-treated samples, we obtained similar inhibitions of $78.2 \pm 9.2\%$; ($n = 11$) and $76.0 \pm 14.2\%$ ($n = 11$) for Bacteria and Thaumarchaeota, respectively (Table 4).

GC7-treatments resulted in an IE for Bacteria of $47.3 \pm 9.5\%$ ($n = 12$) and of Thaumarchaeota of $59.9 \pm 24.7\%$ ($n = 8$) throughout the water column. The lowest inhibition of 25.0% was found in the NSDW (Table 4). The IE of GC7 for Thaumarchaeota was highest in the SSL $77.6 \pm 14.5\%$ ($n = 3$), decreased towards the O₂-min and ULSW to $49.1 \pm 28\%$ ($n = 4$) and was 50% in the NSDW of the Arctic Ocean (Table 4).

To obtain a quantitative measure for the specificity of both inhibitors towards its target group, the inhibition specificity (IS) was calculated (see Material and Methods formula 3). We assumed for EMY, that Bacteria would be the target group, while for GC7, Archaea was the target group. In cases where the amendment of the antibiotic resulted in higher activities than in the control, the negative IE values were excluded to maintain meaningful IS values. Overall, this was assessed only in eight cases, two times using EMY and six times using GC7. Summarizing the ratios given in Table 4, we obtained an overall specificity ratio of 0.18 ± 0.68 ($n = 20$) for EMY, indicating that the inhibition of Bacteria was 18% higher than of Archaea. A ratio of 0.89 ± 1.72 ($n = 15$) was determined for GC7, showing that the specificity of GC7 for Thaumarchaeota was 89% higher than for Bacteria (Table 4, Fig. 5).

TABLE 4: Group-specific inhibition efficiency of EMY and GC7 based on the counts of probe-positive active cells (PSA_c) and associated silver-grain halo area (PSA_a).

WM ^a	Stn	EMY (PSA _c)			GC7 (PSA _c)			EMY (PSA _a)			GC7 (PSA _a)		
		<i>Bacteria</i>	<i>Thaumarchaeota</i>	Ratio ^b	<i>Thaumarchaeota</i>	<i>Bacteria</i>	Ratio ^b	<i>Bacteria</i>	<i>Thaumarchaeota</i>	Ratio ^b	<i>Thaumarchaeota</i>	<i>Bacteria</i>	Ratio ^b
SSL	8	63.0	73.3	-0.14	67.2	29.2	1.30	62.4	70.2	-0.11	66.6	49.3	0.39
	12	70.0	53.3	0.31	-33.5	28.5	ND	79.9	57.6	0.39	NA	56.9	ND
	18	-5.5	40.8	ND	72.8	36.9	0.98	88.2	78.7	0.12	NA	54.6	ND
	20	50.7	63.7	-0.20	22.2	-3.4	ND	81.2	90.9	-0.11	94.4	48.7	0.94
	22	12.3	18.8	-0.34	49.8	45.3	0.10	90.3	95.4	-0.05	69.9	47.7	0.47
O ₂ -min	8	NA	NA	NA	78.7	10.2	6.71	NA	NA	NA	81	56	0.44
	12	62.3	6.7	0.03	NA	NA	NA	81.8	85.7	-0.05	NA	NA	NA
	20	43.7	66.6	-0.34	45.5	21.8	1.08	63.6	76.0	-0.16	27	34	-0.23
	22	51.6	21.5	1.40	5.8	26.2	-0.78	83.2	53.8	0.55	25	54	-0.55
ULSW	8	NA	NA	NA	35.0	18.0	0.94	NA	NA	NA	65	42	0.54
	12	22.5	6.3	2.56	-151.7	40.0	ND	83.4	81.2	0.03	-145	53	ND
	20	38.2	51.9	-0.26	-519.0	-2.1	ND	75.9	87.5	-0.13	-252	46	ND
NSDW	22	9.7	-61.4	ND	-23.4	29.7	ND	70.3	58.8	0.20	50	25	1.00

^a For abbreviation of water masses see Table 1. ^b Ratio – calculated inhibition specificity (for details see material and methods formula 3). Positive ratios indicate an enhanced inhibition of the target (TG), whereas negative ratios imply higher inhibition of the non-target group (NTG). NA – No data. ND – ratio not determined, if negative inhibition efficiencies were obtained, owing to a lower PSA in the control than in the treatment.

Figure 5 shows an overview of the summarized IS ratios given in Table 4 for EMY and GC7. The IS ratios of EMY for both calculation approaches imply a relatively low specificity of the inhibitor. The most abundant ratios were found in the class 0 indicating that the target group and the non-target group were affected similarly by EMY (Fig. 5A). In this summary GC7 revealed a slightly enhanced IS towards the target group, since most IS ratios were found in the classes 0.5 – 1.5 (Fig. 5B). To our knowledge, a common guideline about the specificity of inhibitors is unavailable. Therefore, we defined a specific inhibition, if the IS ratio was >1.0 , meaning that the inhibition of the TG was $>100\%$ higher than the non-target group. An unspecific inhibition was determined if the IS ratio was between ± 1.0 , while an IS ratio of 0 implies that the respective inhibitor revealed an equal specificity regardless of the target group or the non-target group.

An ANOVA analysis (One Way Repeated Measures ANOVA) considering the ratios of Bacteria to Thaumarchaeota revealed no significant difference between the control and EMY, ($F = 0.32$, $p = 0.59$) or GC7 ($F = 0.26$, $p = 0.63$).

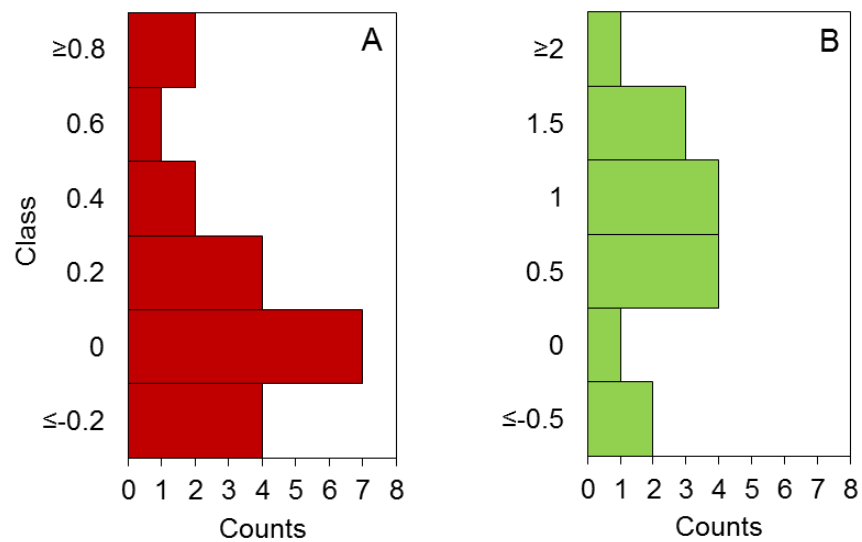


Figure 5: Histogram of specificity ratios grouped into different size classes for EMY (A) and GC7 (B).

DISCUSSION

Liquid scintillation counting and MICRO-CARD-FISH were used to examine the inhibition efficiency (IE) and specificity (IS) of EMY and GC7 on natural prokaryotic assemblages throughout the water column of the North Atlantic. The hybrid method MICRO-CARD-FISH allows the assessment of group-specific leucine incorporation rates at single-cell resolution in addition to examine specific community compositions.

The contribution of Bacteria to total DAPI counts in our study ranged from 29% to 41%, similar to the relative bacterial abundance of 30% reported from a large transect in the North Atlantic (Teira et al. 2006a). The contribution of Thaumarchaeota ranged from 11% to 23% and increased with depth, as reported by other authors (Karner et al. 2001; Church et al. 2003). In earlier studies of the eastern North Atlantic, Thaumarchaeota were found to contribute between 10% and 54% (Yokokawa et al. 2012; Teira et al. 2006a), thus our results are within the range of other reports.

In general, the total recovery efficiency as the sum of probe positive bacterial and archaeal cells from total DAPI counts ranged from 44.5% to 69.2%, obtained with MICRO-CARD-FISH (Fig. 2). Such a discrepancy between probe positive cells and total DAPI counts might be caused due to insufficient cell-wall permeabilization, preventing the diffusion of HRP-labeled oligonucleotide probes into the cells (Wagner et al. 2003). Moreover, it should be noted that several sequence variations of specific probe target sites do exist, prohibiting a group coverage of 100% (Daims et al. 1999; Amann & Fuchs 2008). However, the relatively low abundance of DAPI-stained cells of 37% after microautoradiography highlights the critical step of filter peeling (Fig. S1A). Nevertheless, the ANOVA analysis conducted with the ratio number of probes to DAPI counts between the control and each treatment (EMY and GC7) revealed no significant difference. According to these results no specific cell loss due to the inhibitor treatments or the filter peeling occurred. Thus, we assume that the cell loss occurred randomly supporting the reliance and reproducibility of our reported results.

The concentration and latency experiments measured on the bulk community revealed a substrate incorporation of 111.8 nmol leu m⁻³ d⁻¹ in the control, while 0.7 mmol L⁻¹ EMY-treated samples revealed 25.8 nmol leu m⁻³ d⁻¹ and 1 mmol L⁻¹ GC7 showed 64.1 nmol leu m⁻³ d⁻¹. Yokokawa et al. (2000) used a lower concentration of EMY of 0.15 mmol L⁻¹ with a pre-incubation time of 30 min and reported leucine incorporations in the range of 0.1 to 47.2 nmol leu m⁻³ d⁻¹ which is up to ~55% higher than the leucine incorporation of the 0.7 mmol L⁻¹ treatment reported in this study. We obtained lower leucine incorporation rates in both

treatments probably indicating a better inhibition due to increased concentrations and a longer pre-incubation time. Furthermore, the inhibition of the bulk community with EMY was always higher compared to the inhibition of GC7 (Fig. 3B), which is in agreement with the findings of Yokokawa et al. (2012).

The combination of EMY and GC7 revealed a leucine incorporation which was higher than the uptake rates of EMY-treated samples. Generally, most microorganisms are susceptible to antibiotics (Wilson 2014) although multidrug resistance is assumed to be widespread (Kohanski et al. 2010; Dunkle et al. 2010). More specifically, for a variety of pathogenic Bacteria single and multidrug resistance has been reported (Levy & Marshall 2004). Such resistance mechanisms against EMY and or GC7 might explain the relatively high remaining leucine incorporation rates of samples treated with the inhibitors (Fig. 4B and Fig. 4C). Furthermore, several isolated soil *Bacteria* are able to metabolize antibiotics as their sole carbon source (Dantas et al. 2008). Hence, antibiotic resistant microorganisms might be able to assimilate the inhibitor which could explain to some extent the higher leucine incorporation rates of samples treated with either EMY or GC7 compared to the unamended controls (Table 2, Table 3, Table 4). In general, such discrepancies have been found more frequently in GC7-treated samples than in samples spiked with EMY. According to Jansson et al. (2000) GC7 causes a reversible inhibition of archaeal cell growth, thus the polyamine could also stimulate the growth of resistant microorganisms. However, the effects of a drug combination on bacterial survival are manifold ranging from additive, synergistic to antagonistic (Kohanski et al. 2010). Thus, we cannot exclude a suppression interaction (Chait et al. 2007; Kohanski et al. 2010) between EMY and GC7. This might additionally explain the slightly higher leucine incorporation of the bulk community found in the combined treatment of EMY and GC7 compared to the single treatments (Fig. 3A).

Considering the bulk inhibition alone, it seems that the substrate uptake of the bulk community treated with GC7 represents the bacterial and EMY-treated samples the archaeal fraction (Fig. 3B). This assumes a similar substrate affinity of Bacteria and Archaea, a community composition that is dominated by Bacteria (~80%) rather than by Archaea (20%) and additionally that both inhibitors are truly group-specific. However, comparing the results of Figure 3B with Table 3 and Figure 4 these assumptions, particularly in terms of group specificity, seem to be rather unlikely. To clarify these statements in more detail, we determined both, the group-specific inhibition efficiency and specificity of both inhibitors.

The inhibition efficiency (IE) assessed with EMY for Bacteria was 61% indicating that the bacterial metabolism is affected, although the IE seems to be lower than previously

assumed by Yokokawa et al. (2012) who reported inhibitions ranging from 81% at 200 m to 91% at 300 m depth. Archaea seem to be susceptible to EMY since the activity of Thaumarchaeota was considerably inhibited by ~62%. EMY should specifically inhibit the bacterial protein synthesis (Wilson 2014), whereas Eukaryotes and Archaea should remain unaffected (Dunkle et al. 2010). Yokokawa et al. (2012) reported a specific inhibition of Bacteria but not of Archaea due to EMY using a concentration 0.15 mmol L^{-1} . Nevertheless, the interaction between EMY and the 50S ribosome is primarily structure dependent but to a certain extent also affected by the concentration of the antibiotic (Dunkle et al. 2010). Thus, under relative high concentrations archaeal ribosomes may be a potential target site, apparently reflected by the unspecific inhibition pattern obtained during this study, since samples were spiked with a four times higher concentration of EMY (0.7 mmol L^{-1}).

The finding that GC7 caused an inhibition of both Bacteria (39%) and Thaumarchaeota (54%) implies that GC7 is apparently not as specific as previously assumed (Löscher et al. 2012; Berg et al. 2014a). The inhibition specificity ratio of GC7 was 0.88, suggesting that Thaumarchaeota were to 88% more affected than Bacteria. Nevertheless, a relatively high inhibition of the non-target group by GC7 was found in our samples. According to phylogenetic studies, genes encoding for deoxyhypusine synthase (DHS), a crucial enzyme involved in the post-translational modification of initiation factors, are subject of horizontal gene transfer, supposedly from Archaea to Bacteria. However, it remains enigmatic whether Bacteria can make use of those acquired genes (Brochier et al. 2004). Indeed, Jansson et al. (2000) reported a 30% longer doubling time of *E. coli* treated with 1 mmol L^{-1} of GC7. They concluded that an elevated polyamine level within bacterial cells might be responsible for the cell growth delay (Jansson et al. 2000). Similarly, our results also imply that Bacteria are affected by the used concentrations of GC7, although supposedly indirectly due to higher internal polyamine concentrations rather than directly through an interaction between the inhibitor and a specific enzyme, owing to the assumption that the potential target site for GC7 is absent in Bacteria.

Inhibition of archaeal chemoautotrophic activity and N_2O production by GC7 have been reported (Löscher et al. 2012; Berg et al. 2014a,b), however, a detailed evaluation of the group-specific inhibition was not presented. It should be noted that the assessment of inhibition specificities have been generally conducted under experimental conditions and tested with selected model organisms (Kannan & Mankin 2011; Löscher et al. 2012; Berg et al. 2014a). Hence, knowledge about the influence of antibiotics on complex and diverse natural microbial communities is sparse.

Most studies are predominantly based on Bacteria and Eukaryotes, since most human and veterinary pathogens are located within the phyla *Bacteroidetes*, *Firmicutes*, *Alpha-*, *Beta-* and *Gammaproteobacteria* (Eckburg et al. 2003; Sommer et al. 2009). Moreover, no archaeal virulence genes or virulence factors have been found and no archaeal human pathogens are known (Eckburg et al. 2003). Hence, the hitherto reported knowledge about inhibitors is inevitably biased towards Bacteria.

Finally, it should be noted that the MICRO-CARD-FISH approach has inherent limitations. In addition to the lower cell recovery, the activity is estimated by measuring the silver-grain halo as an area, although the ionizing radiation of radiolabeled substrates is emitted in a three-dimensional space. Consequently, we will underestimate the real activity especially if cells are highly active and thus, the calculated inhibitions might be biased towards Bacteria, since the bacterial leucine incorporation was generally higher compared to Thaumarchaeota.

SUMMARY AND CONCLUSIONS

We showed that EMY affected the substrate incorporation of Bacteria and Thaumarchaeota. GC7 inhibited Thaumarchaeota, however, Bacteria were also considerably affected. Taken together, we could show that the dual inhibitor approach using EMY and GC7 is error prone and estimated group specific activity has to be interpreted with caution, at least if applied to natural and complex microbial communities. Furthermore, our results underline the importance to elucidate the inhibition efficiency and specificity of metabolic inhibitors at the single-cell level.

ACKNOWLEDGEMENTS

I would like to thank my supervisor Gerhard J. Herndl for providing me the opportunity to do this MSc thesis, his helpful comments on the manuscript and his compelling lectures about biological and microbial oceanography.

I want to thank Thomas Reinthaler for the introduction to CARD-FISH, for fruitful discussions and his fascinating lecture about biogeochemistry of the ocean.

I am deeply grateful to Alexander H. Frank for the great introduction to MICRO-CARD-FISH, epifluorescence microscopy, data analysis, fruitful discussions, helpful comments on the manuscript and his invested time.

I want to thank Christian Baranyi for his helpful advice, Eva Sintes, Nathalie Elisabeth and Nicole Köstner for their help with CARD-FISH, Maria Pinto for her support during image acquisition.

I want to thank my mother and Oliver for their guidance over the last years and my friends for the great moments spent together.

I am very grateful to Anneliese and Zigo for their support over the last years.

Last but not least, I am deeply grateful to Mariana, who was always inspiring and motivating me, especially during challenging times.

REFERENCES

- Alonso C (2012) Tips and tricks for high quality MAR-FISH preparations: focus on bacterioplankton analysis. *Syst Appl Microbiol* 35:503–12
- Amann RI, Blinder BJ, Olson RJ, Chisholm SW, Devereux R, Stahl D (1990) Combination of 16S rRNA-targeted oligonucleotide probes with flow cytometry for analyzing mixed microbial populations. *Appl Environ Microbiol* 56:1919–25
- Amann RI, Fuchs BM (2008) Single-cell identification in microbial communities by improved fluorescence in situ hybridization techniques. *Nat Rev Microbiol* 6:339–348
- Arístegui J, Gasol JM, Duarte CM, Herndl GJ (2009) Microbial oceanography of the dark ocean's pelagic realm. *Limnol Oceanogr* 54:1501–29
- Berg IA, Kockelkorn D, Ramos-Vera WH, Say RF, Zarzycki J, Hügler M, Alber BE, Fuchs G (2010) Autotrophic carbon fixation in archaea. *Nat Rev Microbiol* 8:447–60
- Berg C, Vandieken V, Thamdrup B, Jürgens K (2014a) Significance of archaeal nitrification in hypoxic waters of the Baltic Sea. *ISME J*. doi: 10.1038/ismej.2014.218
- Berg C, Listmann L, Vandieken V, Vogts A, Jürgens K (2014b) Chemoautotrophic growth of ammonia-oxidizing thaumarchaeota enriched from a pelagic redox gradient in the Baltic Sea. *Front. Microbiol.* 5: 1-10. doi: 10.3389/fmicb.2014.00786
- Brochier CE, López-García P, Moreira D (2004) Horizontal gene transfer and archaeal origin of deoxyhypusine synthase homologous genes in bacteria. *Gene* 330:169–176
- Chait R, Craney A, Kishony R (2007) Antibiotic interactions that select against resistance. *Nature* 446:668–71
- Church MJ, DeLong EF, Ducklow HW, Karner MB, Preston CM, Karl DM (2003) Abundance and distribution of planktonic archaea and bacteria in the waters west of the Antarctic Peninsula. *Limnol Oceanogr* 48:1893–902
- Daims H, Brühl A, Amann R, Schleifer KH, Wagner M (1999) The domain-specific probe EUB338 is insufficient for the detection of all bacteria: development and evaluation of a more comprehensive probe set. *Syst Appl Microbiol* 22:434–44
- Dantas G, Sommer MOA, Oluwasegun RD, Church GM (2008) Bacteria subsisting on antibiotics. *Science* 320:100–3
- Dunkle JA, Xiong L, Mankin AS, Cate JHD (2010) Structures of the escherichia coli ribosome with antibiotics bound near the peptidyl transferase center explain spectra of drug action. *Proc Natl Acad Sci USA* 107:17152–7
- Eckburg PB, Lepp PW, Relman DA (2003) Archaea and their potential role in human disease. *Infect Immun* 71:591–96

- Eiler A (2006) Evidence for the ubiquity of mixotrophic bacteria in the upper ocean: implications and consequences. *Appl Environ Microbiol* 72:7431–37
- Fariás L, Fernández C, Faúndez J, Cornejo M, Alcaman ME (2009) Chemolithoautotrophic production mediating the cycling of the greenhouse gases N₂O and CH₄ in an upwelling ecosystem. *Biogeosciences* 6:3053–69
- Francis CA, Beman JM, Kuypers MMM (2007) New processes and players in the nitrogen cycle: the microbial ecology of anaerobic and archaeal ammonia oxidation. *ISME J* 1:19–27
- Herndl GJ, Reinthaler T, Teira E, Aken V, Veth C, Pernthaler A, Aken H Van, Pernthaler J (2005) Contribution of archaea to total prokaryotic production in the deep atlantic ocean. *Appl Environ Microbiol* 71:2303–9
- Hesselsoe M, Nielsen JL, Roslev P, Nielsen PH (2005) Isotope labeling and microautoradiography of active heterotrophic bacteria on the basis of assimilation of ¹⁴C₂. *Appl Environ Microbiol* 71:646–55
- Hügler M, Sievert SM (2011) Beyond the calvin cycle: autotrophic carbon fixation in the ocean. *Ann Rev Mar Sci* 3:261–89
- Jannasch HW, Wirsen CO (1973) Deep-sea microorganisms: in situ response to nutrient enrichment. *Science* 180:641–43
- Jansson BPM, Malandrin L, Johansson HE (2000) Cell cycle arrest in archaea by the hypusination inhibitor N1-Guanyl-1,7-Diaminoheptane. *J Bacteriol* 182:1158–61
- Kannan K, Mankin AS (2011) Macrolide antibiotics in the ribosome exit tunnel: species-specific binding and action. *Ann NY Acad Sci* 1241:33–47
- Karner MB, DeLong EF, Karl DM (2001) Archaeal dominance in the mesopelagic zone of the pacific ocean. *Nature* 409:507–10
- Kohanski MA, Dwyer DJ, Collins JJ (2010) How antibiotics kill bacteria: from targets to networks. *Nat Rev Microbiol* 8:423–35
- Lee N, Nielsen PH, Andreasen KH, Juretschko S, Nielsen JL, Schleifer KH, Wagner M (1999) Combination of fluorescent in situ hybridization and microautoradiography - a new tool for structure-function analyses in microbial ecology. *Appl Environ Microbiol*. 65:1289-97
- Levipan H, Quiñones R, Urrutia H (2007a) A time series of prokaryote secondary production in the oxygen minimum zone of the humboldt current system, off central chile. *Prog Oceanogr* 75:531–49
- Levipan H, Quiñones R, Johansson HE, Urrutia H (2007b) Methylotrophic methanogens in the water column of an upwelling zone with a strong oxygen gradient off central chile. *Microbes Environ* 22:268–78

- Levy SB, Marshall B (2004) Antibacterial resistance worldwide: causes, challenges and responses. *Nat Med* 10:122–29
- Löscher CR, Kock A, Könneke M, LaRoche J, Bange HW, Schmitz RA (2012) Production of oceanic nitrous oxide by ammonia-oxidizing archaea. *Biogeosciences* 9:2419–29
- Malmstrom RR, Kiene RP, Cottrell MT, Kirchman DL (2004) Contribution of SAR11 bacteria to dissolved dimethylsulfoniopropionate and amino acid uptake in the North Atlantic Ocean. *Appl Environ Microbiol* 70:4129–35
- Marie D, Brussaard CPD, Thyrhaug R, Bratbak G, Vaulot D (1999) Enumeration of marine viruses in culture and natural samples by flow cytometry. *Appl Environ Microbiol* 65:45–52
- Marshall J, Kushnir Y, Battisti D, Chang P, Czaja A, Dickson R, Hurrell J, McCartney M, Saravanan R, Visbeck M (2001) North atlantic climate variability: phenomena, impacts and mechanisms. *Int J Climatol* 21:1863–98
- Morris RM, Rappé MS, Connon SA, Vergin KL, Siebold WA, Carlson CA, Giovannoni SJ (2002) SAR11 clade dominates ocean surface bacterioplankton communities. *Nature* 420:806–10
- Ouverney CC, Fuhrman JA (2000) Marine planktonic archaea take up amino acids. *Appl Environ Microbiol* 66:4829–33
- Owen OE, Kalhan SC, Hanson RW (2002) The key role of anaplerosis and cataplerosis for citric acid cycle function. *J Biol Chem* 277:30409–12
- Park MH, Nishimura K, Zanelli CF, Valentini SR (2010) Functional significance of eIF5A and its hypusine modification in eukaryotes. *Amino Acids* 38:491–500
- Reinthal T, Aken HM van, Herndl GJ (2010) Major contribution of autotrophy to microbial carbon cycling in the deep North Atlantic's interior. *Deep Sea Res Part II* 57:1572–80
- Samo TJ, Smriga SP, Malfatti F, Pedler BE, Azam F (2014) Broad distribution and high proportion of protein synthesis active marine bacteria revealed by click chemistry at the single-cell level. *Front Mar Sci* 1:1–18
- Shiklomanov IA, Rodda JC (2004) World water resources at the beginning of the twenty-first century. Cambridge University Press, The Edinburgh Building, Cambridge (UK)
- Sommer MOA, Dantas G, Church GM (2009) Functional characterization of the antibiotic resistance reservoir in the human microflora. *Science* 325:1128–31
- Swan BK, Martinez-Garcia M, Preston CM, Sczyrba A, Woyke T, Lamy D, Reinthal T, Poulton NJ, Masland EDP, Gomez ML, Sieracki ME, DeLong EF, Herndl GJ, Stepanauskas R (2011) Potential for chemolithoautotrophy among ubiquitous bacteria lineages in the dark ocean. *Science* 333:1296–300

- Teira E, Lebaron P, Aken HM van, Herndl GJ (2006a) Distribution and activity of bacteria and archaea in the deep water masses of the North Atlantic. *Limnol Oceanogr* 51:2131–44
- Teira E, Burg D, Aken HM van, Veth C, Herndl GJ (2006b) Archaeal uptake of enantiomeric amino acids in the meso- and bathypelagic waters of the North Atlantic. *Limnol Oceanogr* 51:60–69
- Teira E, Reinthaler T, Pernthaler A, Pernthaler J, Herndl GJ (2004) Combining catalyzed reporter deposition-fluorescence in situ hybridization and microautoradiography to detect substrate utilization by bacteria and archaea in the deep ocean. *Appl Environ Microbiol* 70:4411–14
- Thauer RK (2007) A fifth pathway of carbon fixation. *Science* 318:1732–33
- Varela MM, Aken HM Van, Sintes E, Herndl GJ (2008) Latitudinal trends of crenarchaeota and bacteria in the meso- and bathypelagic water masses of the eastern North Atlantic. *Environ Microbiol* 10:110–24
- Wagner M, Horn M, Daims H (2003) Fluorescence in situ hybridisation for the identification and characterisation of prokaryotes. *Curr Opin Microbiol* 6:302–309
- Wallner G, Amann R, Beisker W (1993) Optimizing fluorescent in situ hybridization with rRNA-targeted oligonucleotide probes for flow cytometric identification of microorganisms. *Cytometry* 14:136–43
- Wilson DN (2014) Ribosome-targeting antibiotics and mechanisms of bacterial resistance. *Nat Rev Microbiol* 12:35–48
- Woebken D, Fuchs BM, Kuypers MMM, Amann R (2007) Potential interactions of particle-associated anammox bacteria with bacterial and archaeal partners in the Namibian Upwelling System. *Appl Environ Microbiol* 73:4648–57
- Wuchter C, Abbas B, Coolen MJL, Herfort L, Bleijswijk J van, Timmers P, Strous M, Teira E, Herndl GJ, Middelburg JJ, Schouten S, Sinninghe Damsté JS (2007) Archaeal nitrification in the ocean. *Proc Natl Acad Sci U S A* 104:12317–322
- Yokokawa T, Sintes E, Corte D De, Olbrich K, Herndl GJ (2012) Differentiating leucine incorporation of archaea and bacteria throughout the water column of the eastern Atlantic using metabolic inhibitors. *Aquat Microb Ecol* 66:247–56

SUPPLEMENTARY MATERIAL

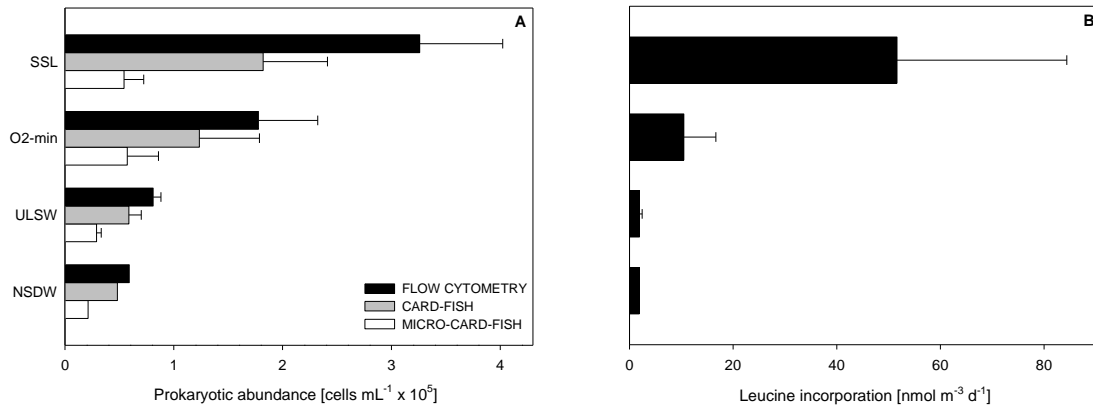


Figure S1: (A) Prokaryotic abundance obtained with flow cytometry, CARD-FISH and MICRO-CARD-FISH. (B) Leucine incorporation of the bulk community. The error bars indicate the standard deviation of the mean values. SSL (n = 5), O₂-min (n = 4), ULSW (n = 3), NSDW (n = 1). For water mass abbreviations see Table 1.

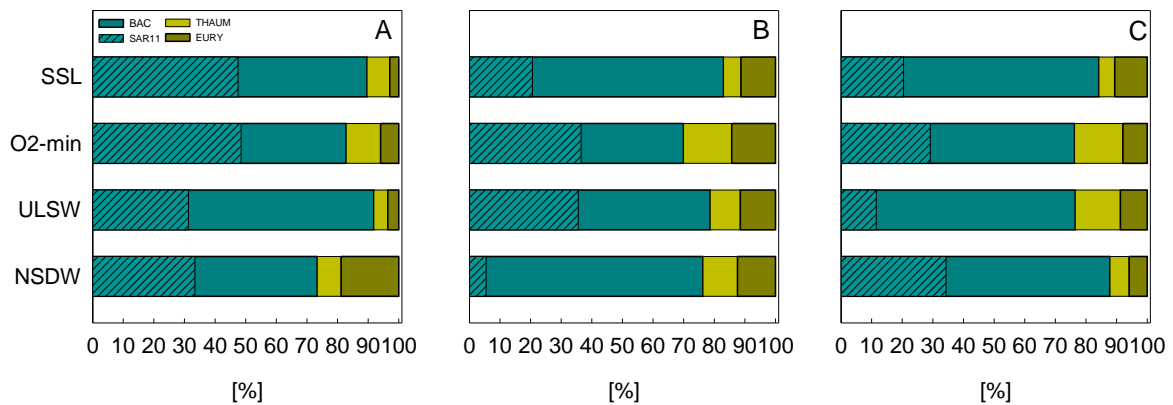


Figure S2: Values given in Figure 4 are up-scaled to 100% in order to increase the readability. (A) Leucine uptake of the control, (B) of EMY and (C) of GC7. For water mass abbreviations see Table 1.

Test of exposure time for microautoradiography

The required exposure time for microautoradiography was tested on two samples with high substrate incorporations of the SSL at station 8. One sample was amended with ^3H -leucine and one with ^{14}C -sodium bicarbonate, liquid scintillation counting revealed an incorporation of $12.4 \mu\text{mol C m}^{-3} \text{d}^{-1}$ and $46.5 \mu\text{mol C m}^{-3} \text{d}^{-1}$, respectively (Fig. S3A and S3B). Additionally, MICRO-CARD-FISH was performed with both samples, after an exposure time of 6 days 53% of DAPI counted cells were active (Fig. S3A), whereas after 29 days just 6% of measured DAPI positive cells were active in the sample spiked with ^{14}C -sodium bicarbonate (Fig. S3B). Thus, an exposure time of 6 days was used for all SSL samples and for the O_2 -min samples of Stn 8, 12 and 22. We decided to extend the exposure time to 8 days for the following water masses and stations (O_2 -min Stn 20, as well as for NSDW Stn 22, ULSW Stn 8, 12, and 20), since a slight decrease of developed silver-grain halos was noticed compared to the tested SSL sample of Stn 8. The ^{14}C -sodium bicarbonate experiments were excluded from further analysis, since the low percentage of active cells. Therefore, we focused on ^3H -leucine to test the inhibition specificity of EMY and GC7 on natural prokaryotic assemblages.

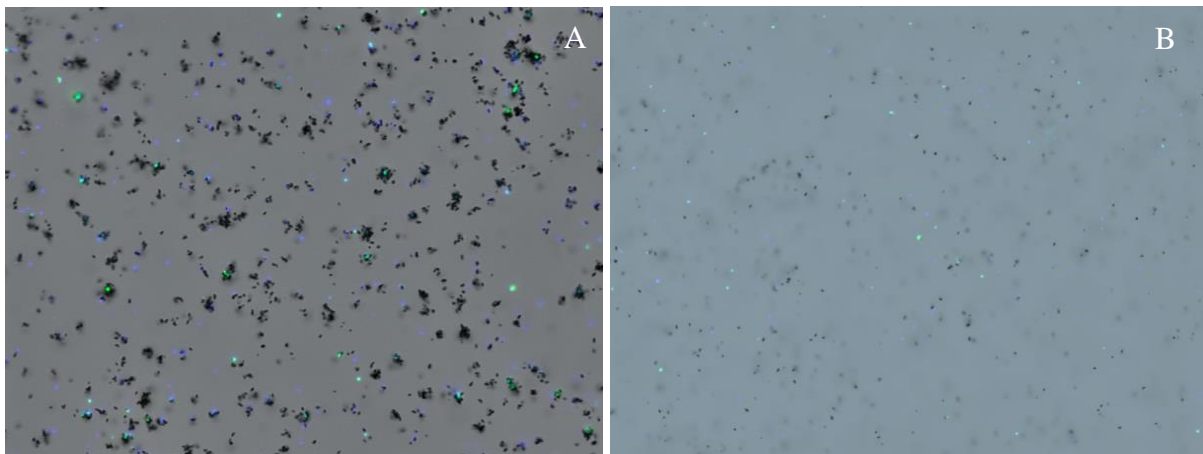


Figure S3: MICRO-CARD-FISH images of different radioactive labeled substrates of SSL samples at Stn 8. (A) ^3H -leucine after 6 days of exposure with a substrate uptake of $12.4 \mu\text{mol C m}^{-3} \text{d}^{-1}$ of the CTRL sample and (B) of ^{14}C -sodium bicarbonate after 29 days of incubation and $46.5 \mu\text{mol C m}^{-3} \text{d}^{-1}$ of the CTRL.

TABLE S1: Overview of bulk- and group-specific leucine incorporations [$\text{nmol m}^{-3} \text{d}^{-1}$] determined in the control and both treatments.

WM ^a	CTRL					EMY					GC7				
	Bulk	Bacteria	SAR11	Thaumarchaeota	Euryarchaeota	Bulk	Bacteria	SAR11	Thaumarchaeota	Euryarchaeota	Bulk	Bacteria	SAR11	Thaumarchaeota	Euryarchaeota
SSL	51.6	46.3	24.5	3.8	1.5	12.0	10.0	2.5	0.7	1.4	27.4	23.0	5.6	1.4	2.9
O ₂ -min	10.5	8.7	5.1	1.2	0.6	2.4	1.7	0.9	0.4	0.3	5.9	4.5	1.7	0.9	0.5
ULSW	1.9	1.8	0.6	0.1	0.1	0.5	0.4	0.2	0.0	0.1	1.2	0.9	0.1	0.2	0.1
NSDW	1.3	1.0	0.4	0.1	0.3	0.4	0.3	0.0	0.0	0.0	0.8	0.7	0.3	0.1	0.0

^a For water mass abbreviations and number of measurements see Table 1. CTRL – Control, EMY – Erythromycin, GC7 – N1-guanyl-1,7-diaminoheptane.

Table S2: Overview of applied horseradish peroxidase oligonucleotide probes for MICRO-CARD-FISH.

Probe	Sequence (5' -3')	Target organisms	Published by	[FA] % ^a
EUB338-I	GCTGCCTCCCGTAGGAGT	Bacteria (most)	Amann et al. (1990)	55
EUB338-II	GCAGCCACCCGTAGGTGT	<i>Planctomycetales</i>	Daims et al. (1999)	55
EUB338-III	GCTGCCACCCGTAGGTGT	<i>Verrucomicrobiales</i> , <i>Chloroflexi</i>	Daims et al. (1999)	55
NON-EUB338	ACTCCTACGGGAGGCAGC		Wallner et al. (1993)	55
SAR11-152R	ATTAGCACAAGTTTCCYCGTGT	<i>SAR 11</i> cluster	Morris et al. (2002)	45
SAR11-441R	TACAGTCATTTCTTCCCGAC	<i>SAR 11</i> cluster	Morris et al. (2002)	45
SAR11-542R	TCCGAACTACGCTAGGTC	<i>SAR 11</i> cluster	Morris et al. (2002)	45
SAR11-732R	GTCAGTAATGATCCAGAAAGYTG	<i>SAR 11</i> cluster	Morris et al. (2002)	45
CREN537	TGACCACTTGAGGTGCTG	<i>Crenarchaea</i>	Teira et al. (2004)	20
CREN554	TTAGGCCCAATAATCMTCCCT	<i>Crenarchaea 554-573</i>	Woebken (2007)	20
EURY806	CACAGCGTTTACACCTAG	<i>Euryarchaeota</i>	Teira et al. (2004)	20

^a FA %: percentage of formamide in the hybridization buffer.

Supplementary References

Amann, R.I., Binder, B.J., Olson, R.J., Chisholm, S.W., Devereux, R., and Stahl, D.A. (1990). Combination of 16S rRNA-targeted oligonucleotide probes with flow cytometry for analyzing mixed microbial populations. *Applied and environmental microbiology* 56:1919-1925

Daims, H., Brühl, A., Amann, R., Schleifer, K.-H., and Wagner, M. (1999). The domain-specific probe EUB338 is insufficient for the detection of all bacteria: development and evaluation of a more comprehensive probe set. *Systematic and Applied Microbiology* 22:434-444

Morris RM, Rappé MS, Cannon SA, Vergin KL, Siebold WA, Carlson CA, Giovannoni SJ (2002) SAR11 clade dominates ocean surface bacterioplankton communities. *Nature* 420:806–810

Teira, E., Reinthaler, T., Pernthaler, A., Pernthaler, J., and Herndl, G.J. (2004). Combining catalyzed reporter deposition-fluorescence in situ hybridization and microautoradiography to detect substrate utilization by bacteria and archaea in the deep ocean. *Applied and environmental microbiology* 70:4411-4414

Wallner, G., Amann, R., and Beisker, W. (1993). Optimizing fluorescent in situ hybridization with rRNA-targeted oligonucleotide probes for flow cytometric identification of microorganisms. *Cytometry* 14:136-143

Woebken, D., Fuchs, B.A., Kuypers, M.a.A., and Amann, R. (2007). Potential interactions of particle-associated anammox bacteria with bacterial and archaeal partners in the Namibian upwelling system. *Applied and environmental microbiology* 73:4648-4657

ZUSAMMENFASSUNG

Die Verwendung von Inhibitoren, die spezifisch den Metabolismus von Bakterien und Archaeen inhibieren, ist hilfreich um gruppenspezifische Aktivitäten zu messen. Im Zuge dieser Arbeit testeten wir die Inhibierungsspezifität von Erythromycin (EMY) und N1-guanyl-1,7-diaminoheptan (GC7) an Prokaryoten des offenen Ozeans, die bis dato noch nicht in diesem Umfang durchgeführt worden ist. Wir stellten die Hypothese auf, dass EMY behandelte Proben die Produktivität der Archaeen repräsentieren, wohingegen GC7 behandelte Proben als guter Proxy der bakteriellen Aktivität angesehen werden können. Wasserproben wurden im Juni und Juli 2012 aus verschiedenen Tiefen im Nordatlantik genommen. Die Inhibierung der ^3H -Leucin Aufnahme wurde mit Hilfe von Catalyzed Reporter Deposition Fluorescence *In Situ* Hybridisierung in Kombination mit Mikroautoradiographie (MICRO-CARD-FISH) und Flüssigszintillationszähler gemessen. Des Weiteren wurden Durchflusszytometrie, CARD-FISH und MICRO-CARD-FISH angewendet, um die mikrobielle Abundanz und die Zusammensetzung der mikrobiellen Gemeinschaft zu bestimmen. Die mikrobielle Abundanz nahm mit der Tiefe exponentiell ab, von 3.3×10^5 zu 8.1×10^4 Zellen mL^{-1} . Die Leucin-Aufnahme korrelierte gut mit der mikrobiellen Abundanz und schwankte zwischen 51.6 und 1.9 $\text{nmol Leucin m}^{-3} \text{d}^{-1}$. Gemessen an DAPI-Zählungen, schwankte der Anteil an Bakterien zwischen 28.6 und 46.5%, während SAR11 zwischen 12.2 und 20.8% ausmachte. Gemessen an gesamten DAPI-Signalen machten Thaumarchaeen zwischen 10.5 und 23.2% und Euryarchaeen zwischen 2.3 und 11.5% aus. Entgegen bisheriger Annahmen, führte EMY zu einer vergleichbaren Inhibierung der Leucin-Aufnahme von Bakterien und Archaeen (~61%). GC7 reduzierte die Substrataufnahme, ähnlich wie EMY, allerdings war die ^3H -Leucin-Aufnahme der Bakterien zu 39% und die der Archaeen zu 54% reduziert. Wir schlussfolgern daher, dass der getestete Doppelte-Inhibierungsansatz scheinbar zu unspezifisch ist, um damit die Aktivität von Bakterien und Archaeen im offenen Ozean unterscheiden zu können.

CURRICULUM VITAE

PERSONAL INFORMATION

Name: **Benjamin Pontiller**

Nationality: Austrian

EDUCATION

- 05/2015 - 03/2013 **MSc in Ecology with main focus on Marine Biology, Microbial Oceanography**, University of Vienna, Department of Limnology and Biological Oceanography, Centre of Ecology, University of Vienna, Althanstraße 14, 1090 Vienna, Austria
- 02/2013 - 10/2009 **BSc in Biology**, University of Vienna, Althanstraße 14, 1090 Vienna, Austria
- 05/2009 **General qualification for university entrance (BRP)**, BFI Tyrol - Lienz, Beda Weber-Gasse 20, 9900 Lienz, Austria
- 09/2007 **External exam – Biology and Environmental Study**, Academic high school for employed persons (BG/BRG)- Adolf Pichler Platz 1, 6020 Innsbruck, Austria
- 12/2006 - 04/2006 **Alternative civilian service**, Austrian Red Cross, Emanuel Hibler-Straße 3a, 9900 Lienz, Austria
- 04/2006 - 09/2005 **College for Mechanical Engineering and Automation**, Private Higher Technical Institute Lienz (PHTL), Linker Iselweg 22, 9900 Lienz, Austria
- 05/2005 - 09/2001 **Technical College for Mechanical Engineering**, Higher Technical Institute (HTL), Lastenstraße 1, 9020 Klagenfurt, Austria

RESEARCH ACTIVITIES / INTERNSHIPS

- Master Thesis at the Department of Limnology and Biological Oceanography (2014 – 2015)
Title: „Usage of metabolic inhibitors to quantify bacterial and archaeal activity in meso- and bathypelagic waters of the North Atlantic“ (Supervisor: Univ.-Prof. Dr. Gerhard J. Herndl)
- Practical Course in Molecular Microbiology, Microbial Ecology and Immunobiology - Austria (WS-2013)
- Bioinformatics for Metagenomics and Metatranscriptomics (WS-2013)
- Planning and Analysis of Multivariate Experiments in Ecology (WS-2013)
- Practical Course in Marine Ecology - Slovenia (SS-2013)
Title: „*In vivo* salinity experiments of *Zoothamnium niveum* living in thiotrophic symbiosis and recruitment experiments of peritrich ciliates in an estuarine environment in the northern Adriatic Sea“ (Supervisor: Univ.-Prof. Dr. Monika Bright)
- Fluoreszenz-*In-Situ*-Hybridization (FISH) - Austria (WS-2012)
- Introduction to the Fauna and Flora of Marine Habitats - Croatia (SS-2012)
- Functional Ecology of Rainforests - Field course - Costa Rica (WS 2011)
- Bachelor Thesis at the University of Vienna, Sea Turtle Project - Field course - Turkey (SS 2011)
Title: „Sand temperature change through shadow in a *Caretta caretta* breeding area at Calis, Fethiye, Turkey“ (Supervisor: Doz. Dr. Michael Stachowitsch)
- Practical Course in Functional Ecology - Austria (SS-2011)
- Introduction to Marine Biology - Slovenia (SS-2011)

SKILLS AND QUALIFICATIONS

- Fluorescence *-In-Situ*-Hybridization (FISH)
- Microautoradiography in combination with Catalyzed Reporter Deposition Fluorescence-*In-Situ*-Hybridization (MICRO-CARD-FISH)
- Quantitative PCR (qPCR)
- 16S rRNA full-cycle approach
- Microsoft Office, Sigma Plot, R (basic knowledge)

LANGUAGES

- German (mother tongue)
- English (fluent written and spoken)

PUBLICATIONS

- Frank, H.A., Pontiller, B., Herndl, J. G., Reinthaler, T. 2015. No specific inhibition of Bacteria and Archaea through erythromycin and GC7. *Frontiers in Marine Science* (in preparation).